# CORRELATION OF FINITE-ELEMENT STRUCTURAL DYNAMIC ANALYSIS WITH MEASURED FREE VIBRATION CHARACTERISTICS FOR A FULL-SCALE HELICOPTER FUSELAGE

Irwin J. Kenigsberg
Supervisor - Airframe Dynamics
Sikorsky Aircraft
Stratford, Connecticut

Michael W. Dean
Dynamics Engineer
Sikorsky Aircraft
Stratford, Connecticut

Ray Malatino
Helicopter Loads and Dynamics Engineer
Naval Air Systems Command
Washington, D. C.

## Abstract

Both the Sikorsky Finite-Element Airframe Vibration Analysis Program (FRAN/Vibration Analysis) and the NASA Structural Analysis Program (NASTRAN) have been correlated with data taken in full-scale vibration tests of a modified CH-53A helicopter. With these programs the frequencies of fundamental fuselage bending and transmission modes can be predicted to an average accuracy of three percent with corresponding accuracy in system mode shapes.

The correlation achieved with each program provides the material for a discussion of modeling techniques developed for general application to finite-element dynamic analyses of helicopter airframes. Included are the selection of static and dynamic degrees of freedom, cockpit structural modeling, and the extent of flexible-frame modeling in the transmission support region and in the vicinity of large cut-outs. The sensitivity of predicted results to these modeling assumptions is discussed.

## Introduction

Helicopter vibration and resulting aircraft vibratory stress can lead to costly schedule slippages as well as to problems in field service maintenance and aircraft availability. At the core of vibration control technology is the requirement to design the helicopter structure to minimize structural response to rotor excitations. Both the complexity of the structure and the increasingly stringent mission and vibration control specifications demand development of airframe structural vibration analyses that can be used rapidly and economically to evaluate and eliminate vibration problems during the preliminary design phase of helicopters.

The complex helicopter structure consists of sections that differ considerably in structural arrangement and load carrying requirements. These sections include the cockpit, cabin, tail cone, and tail rotor pylon. In addition, large fuselage cut-outs and concentrated masses such as the transmission, main rotor, and tail rotor, which are unique to helicopters, play a major role in controlling vibrations.

Although advanced analytical methods based on finite-element techniques have been developed for studying the vibration characteristics of complex structures, a detailed correlation of such methods with test data is not available in the general literature. Further, little information is available on the accuracy of various modeling assumptions that might be made to reduce the cost and time of applying these vibration analyses.

As a result a research project was establish- by Naval Air Systems Command with Sikorsky Aircraft to:

a) Determine the accuracy of the Sikorsky Finite-Element Airframe Vibration Analysis in predicting the vibration characteristics of complex helicopter airframe structures.

and

b) Develop and evaluate general helicopter dynamic modeling techniques that could be used to provide accurate estimates of vehicle dynamic characteristics while at the same time minimizing the complexity and cost of the analysis.

Due to the increased usage of NASTRAN throughout the industry as well as the efficiency resulting from employing a single analytical system for both static and dynamic analyses, a parallel correlation study using NASTRAN has been performed. The results of these correlation studies are the subject of this paper.

## Phase I - Stripped Vehicle

### Test Vehicle

At the initiation of this effort, the philosophy guiding the development of modeling techniques was based upon the concept of gradually increasing the complexity of the analytical representation. It was decided that the first

Presented at the AHS/NASA-Ames Specialists' Meeting on Rotorcraft Dynamics, February 13-15,1974

correlation study would be conducted on an aircraft stripped of all appendages. It was believed that the modeling techniques for representing airframe response characteristics could be identified and developed most easily in this manner. Then, as various appendages were added to the basic vehicle, only the modeling techniques required for the structure or masses added need be developed.

The vehicle used in this test and correlation study was the CH-53A Tie Down Aircraft, Vehicle designation number 613. A general arrangement of the structure is illustrated in Figure 1. For initial correlation, all appendages were removed. These included the nose gear, main landing gear, main landing gear sponsons, fuel sponsons, tail pylon aft of the fold hinge, tail rotor and associated gear boxes, engines, cargo ramp door, horizontal stabilizer, and all remaining electrical and hydraulic systems. The main rotor shaft and all gears were removed from the main transmission housing and only the housing itself was retained for the test configuration.

## Testing

The ground test facility employed to establish the dynamic characteristics of the test vehicle was a bungee suspension system that simulates a free-free condition, a rotorhead-mounted unidirectional shaker, and the Sikorsky shake test instrumentation console. Instrumentation consisted of 14 fixed and 10 roving accelerometers. A complete description of the test apparatus and the instrumentation is provided in Reference 1.

All accelerometer signals and the reference shaker contactor signal were transmitted to the console. The signals were processed automatically by the console resulting in a calculation of the in-phase and quadrature components of the accelerations. The accelerations were then normalized to the magnitude of the shaker force at the particular frequency. As frequency was varied, the resulting response of each accelerometer was recorded on a XYY' plotter, Figure 2, as g's/1000 lbs. versus frequency.

Ideally, a fuselage mode can be identified by a peak in the quadrature response and a simultaneous zero crossing of the in-phase response. Once a mode is located, all quadrature responses at this frequency can be recorded to define the mode shape. The modes defined in this manner from the shake tests are listed in the left-hand column of Table I. It should be noted that this technique is applied more easily at lower frequencies, where sufficient modal separation exists so that the forced response in the vicinity of a resonance is dominated by a single mode. As shown in Figure 2, the mode shapes at higher frequencies must be extracted from the coupled response of many modes.

## Analysis and Correlation

The shake test data indicated that the natural modes of vibration of a helicopter can be categorized as beam-like modes controlled by overall fuselage characteristics (e.g., length, depth, overall bending stiffness, mass distribution, etc.) and those controlled by the transmission support structure. Therefore, the overall helicopter structure was modeled utilizing three modules:

1) center section including the transmission support region

2) forward fuselage and cockpit

and

3) aft fuselage and tail.

The center section was modeled in greatest detail by applying finite-element techniques. The structural characteristics of the forward and aft fuselage were derived from beam theory. These equivalent beams were located at the neutral axis of the airframe section and were assigned the bending and torsional properties of the total section. The beam models of the forward and aft fuselage were cantilevered from rigid frames at the respective forward and aft ends of the center section, Figure 3. The influence coefficients of these beams with respect to their cantilevered ends were then combined with the influence coefficient matrix of the remaining structure.

The Phase I correlation was performed using the Sikorsky Finite-Element Airframe Vibration Analysis (FRAN/Vibration Analysis). This analysis consists of two programs: PPFRAN and a 200 dynamic-degree-of-freedom eigenvalue/eigenvector extraction procedure. PPFRAN is derived from the IBM/MIT Frame Structural Analysis Program, FRAN (Reference 2), a stiffness method, finite-element analysis limited to two types of elements, namely bending elements (bars) and axial elements (rods). This limitation necessitated further development of FRAN for application to stressed skin structures. This development consists of the addition of pre- and post-operative procedures linked to FRAN. In the pre-operative procedure (Pre-FRAN), the fuselage skin is transformed into equivalent rod elements. This transformation is developed by satisfying the criterion that the internal energy of the skin structure under an arbitrary set of loads be the same as that of the transformed structure under the same set of loads. The post-operative procedure (Post-FRAN) extracts the influence coefficient matrix corresponding to the selected dynamic degrees of freedom. A detailed description of the FRAN/Vibration Analysis is provided in Reference 1.

The elements used to represent the airframe structure are:

1) bending (bar) elements for fuselage frames and for the nose and tail beams

2) axial (rod) elements for the stringers

and

3) equivalent, diagonal rod elements for skin panels.

For dynamic analysis, the structure is assumed to be unbuckled, so that all skin panels are considered fully effective in resisting axial loads. Thus, the total axial area of each skin panel is lumped with the areas of adjacent stringers.

During Phase I correlation, three modeling parameters were varied: the number of bays over which the finite-element (flexible-frame) model extends (Figure 4), the number of nodes per frame (number of stringers), and the number of dynamic degrees of freedom assigned to each frame (Figure 5). The results of the correlation are presented in Table I, which shows the sensitivity of the analysis to each of the above parameters and the accuracy of the predicted frequencies and mode shapes. The criteria for establishing the level of mode shape correlation are:

E (Excellent) - Correct number of nodes, nodes less than 2.5 percent of fuselage length from measured location, local modal amplitudes within 20 percent of test values.

G (Good) - Correct number of nodes, nodes less than 2.5 percent of fuselage length from measured location, difference between actual and predicted local modal amplitudes exceeds ±20 percent of test values.

F (Fair) - Correct number of nodes, nodes more than 2.5 percent of fuselage length from measured location, difference between actual and predicted local modal amplitudes exceeds ±20 percent of test values.

P (Poor) - Incorrect number of nodes, nodes located improperly, difference between actual and predicted local modal amplitudes exceeds ±20 percent of test values.

A comparison of the 30- and 60-stringer analyses indicates that there is no change in the results when modeling the structure with half the number of actual stringers. In addition a comparison of results obtained with the basic and reduced dynamic degree of freedom allocation indicates that no more than 16 dynamic degrees of freedom per frame are required for dynamic modeling.

Although mode shape correlation resulting from the analysis in the frequency range of interest (below 1500 cpm) is encouraging, see Table I, the absence of a representative mass distribution made the analysis overly sensitive to certain modeling assumptions. This sensitivity appears to account for the less than satisfactory frequency correlation. For example, the frequency of the transmission pitch mode is normally controlled by the mass of the fully assembled transmission and the properties of the structure in the transmission support region. In the absence of a mass distribution representative of a fully assembled vehicle, however, any element of the structure and any lumped mass can contribute significantly to the control of the dynamic characteristics. In this case, the analytical representation appears to be too stiff because of the beam model used for the fuselage forward of F.S. 262, which constrains the upper and lower decks to deform equally. This constraint is not imposed by the actual structure. A comparison of the results of the 9- and 18-bay analyses indicates that due to the local nature of the transmission pitch mode, extension of the flexible-frame model aft beyond the limit of the 9-bay model has no significant effect on the prediction of this mode.

The poor frequency correlation for the first lateral bending mode persisted throughout this phase of correlation. This mode was characterized by differential shearing of the upper and lower decks of the aft cabin, Figure 7. The 6-bay and 9-bay flexible-frame model represented most of this structure experienceing the differential shearing as a beam capable of only bending and torsion. This overly constrained model resulted in predicted frequencies substantially higher than test values. Extending the flexible-frame representation to 18-bays appears to be the solution. However, size limitations in PPFRAN required that the 18-bay flexible-frame model be generated in two 9-bay substructures, married at a rigid intermediate frame at F.S. 442, Figure 3. Although the extended model improved the correlation of the first lateral bending mode, absence of a representative mass distribution again appears to make the model overly sensitive to the presence of the rigid frame at F.S. 442. This accounted for the remaining difference between test and analysis.

Many of the higher frequency modes are controlled by the structure in the area of the rear cargo ramp. This accounts for the failure to predict the Transmission Vertical mode until the flexible-frame model was extended into the ramp area, see Table I. Although this extension of the model improved correlation, the high frequency modes above 1500 cpm are difficult to identify analytically due to the coupling of overall fuselage modes with local frame modes. This difficulty is compounded in this investigation, because the frequencies of the basic fuselage modes are raised due to the stripped condition of the vehicle, while frequencies of the local frame modes are lowered due to the lumped-mass modeling used to represent each frame. Tests of a more representatively loaded fuselage can be expected to minimize the problem of mode identification.

From the results of this phase of the correlation, it is concluded:

1) The selection of static degrees of freedom in the flexible frame model can be based on a structural model that contains stringers numbering one half the number of actual stringers.

2) No more than sixteen dynamic degrees of freedom on each flexible frame are required for dynamic analysis. The typical location of

these degrees of freedom is illustrated in Figure 5.

3) Transmission modes can be predicted by a flexible-frame representation of the transmission support region extending about 1.5 transmission lengths forward and aft of the corresponding transmission supports, about 9 bays. If the vehicle contains large cutouts, such as the cargo ramp of the test vehicle, the flexible-frame model should extend through this region as well.

## PHASE II - BALLASTED VEHICLE

### Testing

Shake tests were performed after adding ballast to provide a more realistic representation of a helicopter mass distribution, Figure 6. At the transmission mounting plate, two lead blocks having a total weight of 4570 pounds were mounted so that the mass and pitching moment of inertia of the simulated transmission and rotor head approximated that of the actual CH-53A. At the tail, a 1500-pound block was mounted to simulate the removed tail pylon, stabilizer, and tail rotor. At the nose, a 3000-pound block was mounted on the nose gear trunnion fitting to balance the vehicle.

The natural modes of vibration identified by shake tests are listed in Table II along with the frequencies measured during Phase I. Not only did the ballast succeed in lowering the fuselage modes into a frequency range more representative of that encountered on a fully assembled aircraft, but additional modes were also identified that are strongly controlled by the ballast. In fact, these modes were identified as local modes of the ballast blocks themselves. Due to the complex structural nature of the ballast, Figure 6, these appendages did not lend themselves to simple analytical representations. Therefore, the flexibility of each ballast block was measured by instrumenting both the block and the adjacent airframe structure and then measuring the accelerations occurring at both locations near the modal frequencies of interest. The mass of each ballast block and its absolute acceleration resulted in a force which produced the relative motion between the two instrumented parts. The empirically defined flexibilities of the ballast were then used in the dynamic model.

### Analysis and Correlation

The modeling techniques developed in Phase I of this study were applied to both the FRAN/Vibration Analysis and NASTRAN.

The finite-element model analyzed in Phase II was identical to the 18-bay model analyzed in Phase I, except for adding the mass and structural characteristics of the ballast blocks. The FRAN model was formed with rod and bar elements, as discussed previously, while the NASTRAN model used CROD, CBAR, and CSHEAR elements (Reference 3). As before, all skin panels were assumed fully effective in reacting axial load and this effective area was lumped into the adjacent stringers.

Including ballast to replace removed appendages resulted in a substantial improvement in the correlation, particularly in frequency prediction as shown in Table III. Significantly, ballast eliminated the difficulties identified as sensitivity to modeling assumptions and local frame modes in the absence of representative mass distributions. The average error in predicting the frequencies of fundamental fuselage bending modes and the transmission pitch mode was 3-4% for both the FRAN/Vibration Analysis and NASTRAN. In addition the shape correlation for these modes varied from good to excellent. The analyses also were able to predict accurately the significant changes in the characteristics of the fuselage and transmission modes resulting from the addition of the ballast, Figures 7, 8 and 9. To achieve this degree of correlation, modeling of the ballast flexibilities was required. This modeling was successfully accomplished in the vertical/pitch direction, Figure 10, but did not prove successful in the lateral/torsion direction, Figure 11. The contrast between these two results establishes the ability of finite-element analyses to predict accurately the characteristics of fuselage and transmission modes when the structural data base is defined with sufficient accuracy. Further improvement in the correlation could have been achieved if a more detailed definition of the ballast flexibilities had been acquired from measurements of static deflections.

Reasonable success has been achieved in predicting higher frequency, ramp-controlled modes, Figures 12 and 13. However, some margin does exist for further improvements in shape and frequency prediction. From the standpoint of modeling, it appears that the 200 dynamic degree of freedom limit established in this study is inadequate for predicting the shell-type modes of the cargo ramp structure. In addition, the test procedure employed, namely the use of a single rotorhead shaker, does not provide a means of uncoupling the forced response characteristics of modes at the higher frequencies, Figure 2.

### Conclusions

1. Finite element analyses can predict accurately the frequencies and mode shapes of complex helicopter structures, provided the structural data base is defined accurately.

2. Complete stripping of a vehicle for correlation purposes may make the analysis overly sensitive to normally minor modeling assumptions.

3. Significant changes can be predicted accurately in the character and frequency of fuselage and transmission modes due to changes in mass distributions and structural characteristics.

4. The modeling techniques established by this study can be used during aircraft design regardless of the finite-element analytical system being used.

## Recommendations

1) A full-scale shake test correlation should be performed on a fully assembled flight vehicle to establish and validate modeling techniques for those appendages removed during this study.

2) Appendages not amenable to accurate or economical structural analysis should be tested statically to determine flexibility data required for dynamic analysis.

3) Integrated structural design systems should be developed to couple static and dynamic analyses and thus provide the accurate structural data required for defining vibratory response characteristics as early as possible during aircraft design.

4) Use of additional shaker locations should be incorporated in the test procedure to provide a means of uncoupling higher frequency modes. Alternatively, more sophisticated means of processing shake test data (e.g., system identification techniques described in Reference 4) should be employed.

## References


1) Kenigsberg, I. J., CH-53A FLEXIBLE FRAME VIBRATION ANALYSIS/TEST CORRELATION, Sikorsky Engineering Report SER 651195, March 28, 1973.

2) IBM 7090/7094 FRAN FRAME STRUCTURE ANALYSIS PROGRAM (7090-EC-01X).

3) McCormick, C. W., ed., THE NASTRAN USER'S MANUAL, (level 15), NASA SP-222(01), June 1972.

4) Flannelly, W. G., Berman, A., and Barnsby, R. M., THEORY OF STRUCTURAL DYNAMIC TESTING USING IMPEDANCE TECHNIQUES, USAAVLABS TR 70-6A,B, June 1970.

5) Willis, T., FRAN CORRELATION STUDY, Sikorsky Report SYTR-M-36, July 1969.


## Illustrations

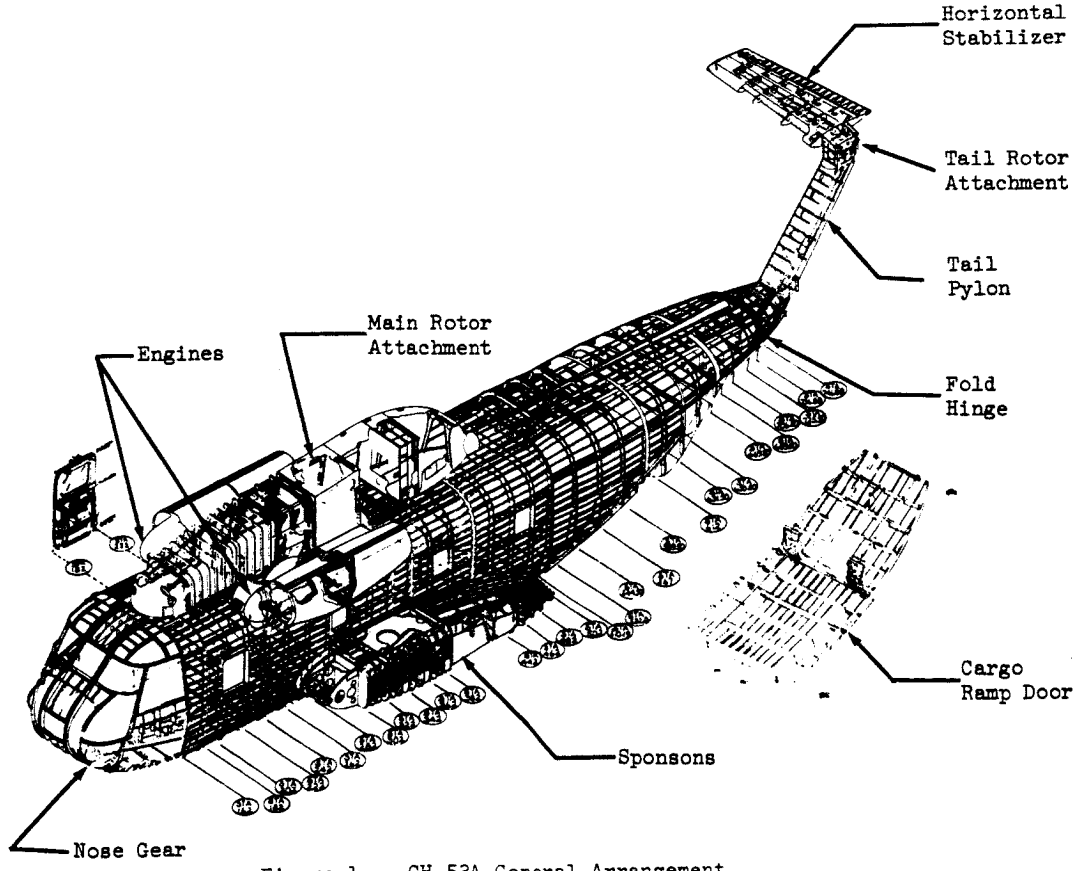


Figure 1 CH-53A General Arrangement

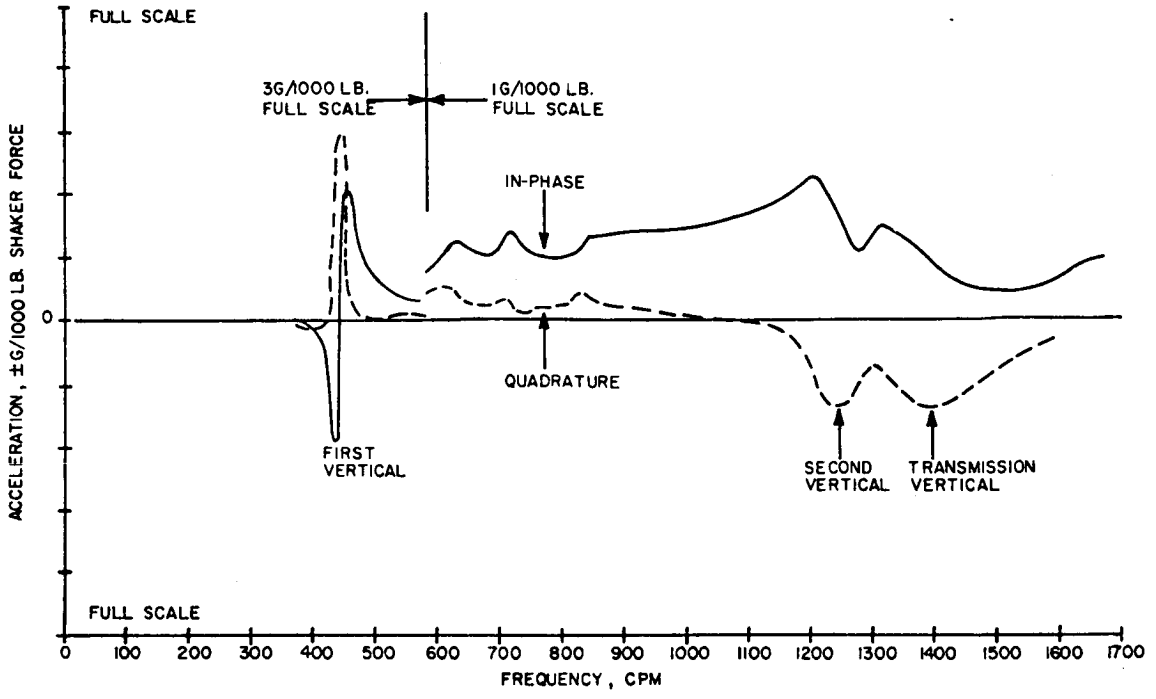


Figure 2 Typical Vertical Response to Vertical Excitation

TABLE I

PHASE I SHAKE TEST CORRELATION SUMMARY

| TEST | | ANALYSIS | | | | | | | | | | | |
|---|---|---|---|---|---|---|---|---|---|---|---|---|---|
| | | 18 Bay 30 Stringer Reduced DOF | | | 9 Bay 30 Stringer Reduced DOF | | | 6 Bay 30 Stringer Reduced DOF | | | 6 Bay 30 Stringer and 60 Stringer Basic DOF | | |
| Mode | Freq. (CPM) | Freq. | Error | Shape | Freq. | Error | Shape | Freq. | Error | Shape | Freq. | Error | Shape |
| 1st Lateral | 910 | 1207 | 33% | G | 1466 | 60% | P | 1435 | 58% | P | 1440 | 58% | P |
| 1st Vertical | 1155 | 1175 | 2% | E | 1282 | 11% | E | 1242 | 8% | E | 1241 | 8% | E |
| XSSN Pitch | 1490 | 1709 | 13% | E | 1710 | 13% | E | 1748 | 17% | E | 1758 | 17% | E |
| 2nd Vertical | 1950 | 2150 | 10% | G | 2390 | 22% | F | 2505 | 28% | F | 2577 | 32% | F |
| XSSN Roll | 2000 | 2405 | 20% | P | 2870 | 43% | P | 2900 | 45% | P | 2894 | 45% | P |
| XSSN Vertical | 2150 | 2250 | 4% | F | | | | | | | | | |
| Torsion | 2300 | 2763 | 20% | F | 2428 | 6% | P/F | 2422 | 6% | P/F | 2445 | 6% | P/F |

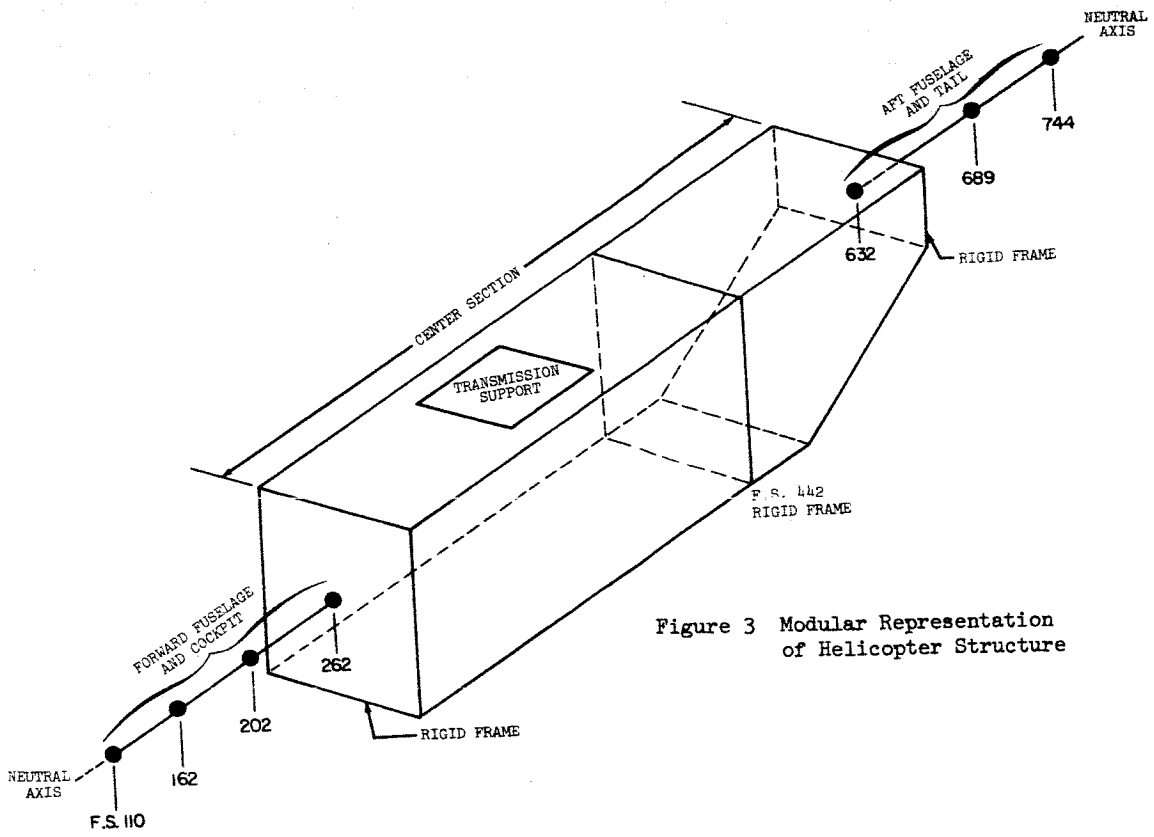


Figure 3 Modular Representation of Helicopter Structure

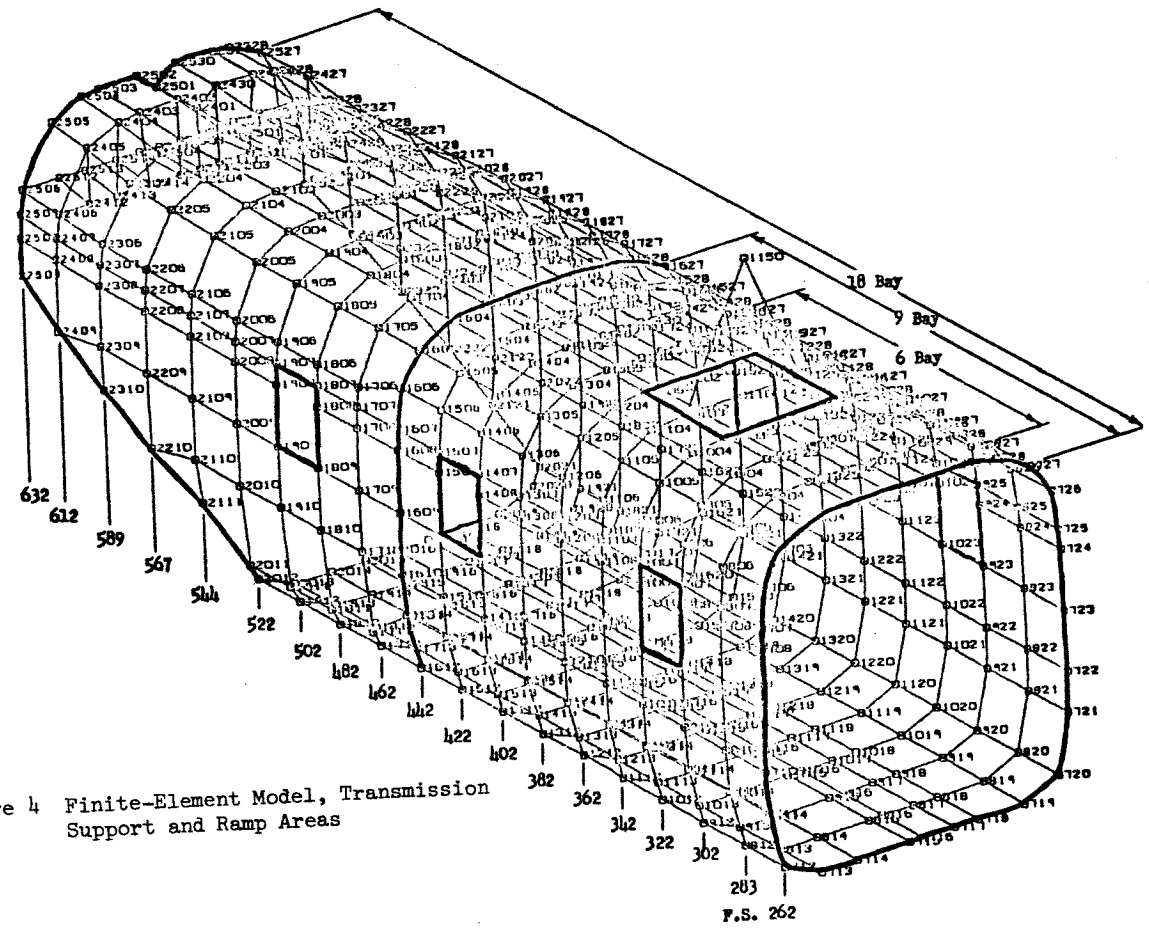


Figure 4 Finite-Element Model, Transmission Support and Ramp Areas

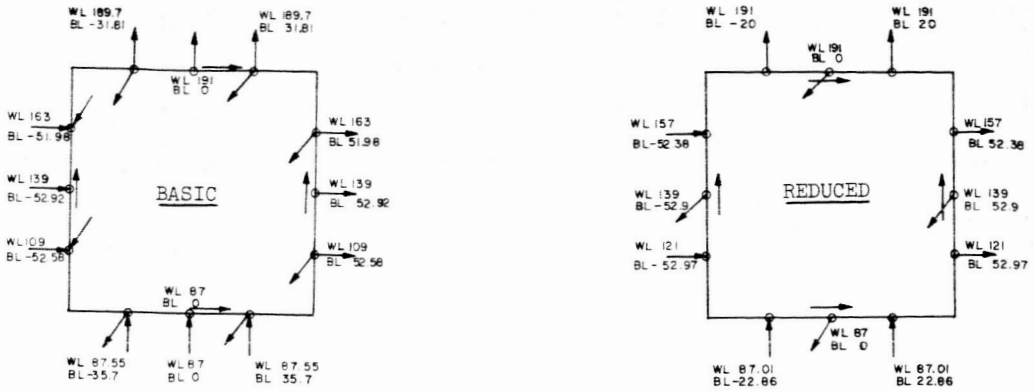


Figure 5 Degree of Freedom Locations for Basic and Reduced Dynamic Degree of Freedom Models

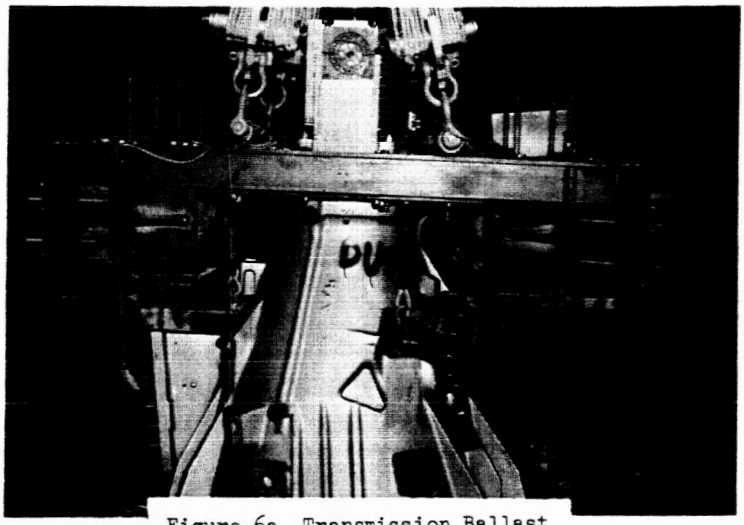

Figure 6a Transmission Ballast Installation

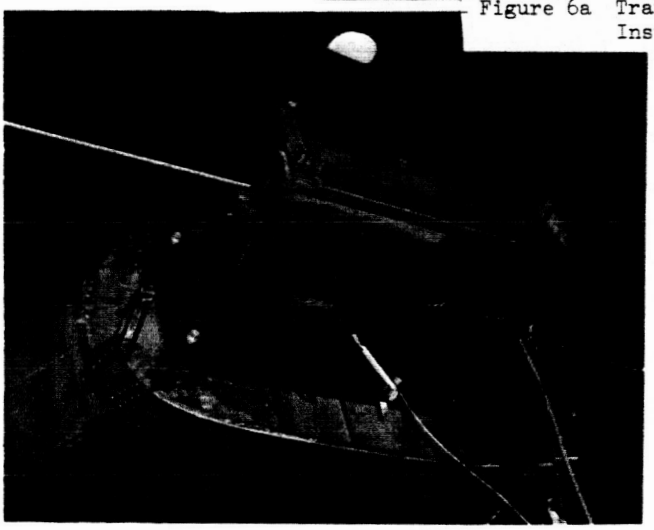

Figure 6b Tail Ballast Installation

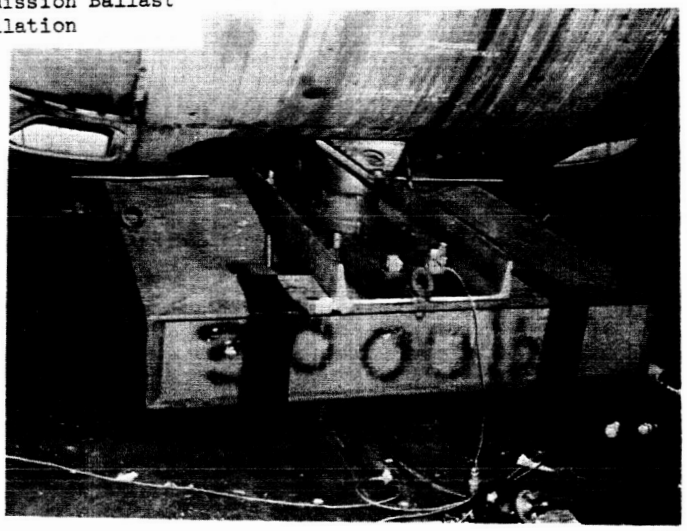

Figure 6c Nose Ballast Installation

Figure 6 Phase II Ballast Installations

TABLE II - SHAKE TEST FREQUENCIES

| MODE | PHASE II TEST FREQUENCY CPM | PHASE I TEST FREQUENCY |
|---|---|---|
| 1st Vertical Bending | 440 | 1155 |
| 1st Lateral Bending | 615 | 910 |
| Transmission Pitch | 740 | 1490 |
| Nose Block Lateral/Roll | 930 | — |
| Nose Block Vertical/Coupled | 970 | — |
| Forward Cabin/Nose Block Lateral | 990 | — |
| Nose Block Vertical | 1050 | — |
| Second Vertical Bending | 1290 | 1950 |
| Torsion | 1310 | 2300 |
| Transmission/Ramp Vertical Bending | 1425 | 2150 |
| Ramp Vertical Bending | 1640 | — |

TABLE III

PHASE II CORRELATION SUMMARY

VERTICAL/PITCH MODES

| MODE | Frequency Test | FRAN | Error | Shape | NASTRAN | Error | Shape |
|---|---|---|---|---|---|---|---|
| 1st Vertical Bending | 440 | 438 | 0% | E | 453 | 3% | E |
| Transmission Pitch | 740 | 751 | 1.5% | G | 785 | 6% | G |
| Nose Block Vertical/ Transmission Pitch | 970 | 933 | 4% | G | 956 | 1.5% | G |
| Nose Block Vertical | 1050 | 1043 | 1% | F | 1063 | 1% | F |
| Second Vertical | 1290 | 1523 | 18% | F | 1608 | 25% | F |
| Transmission Vertical/ Ramp Vertical | 1425 | 1563 | 10% | F/G | 1843 | 29% | F/G |
| Ramp Vertical | 1640 | 1394 | 15% | P/F | 1355 | 17% | P/F |

LATERAL/TORSION MODES

| | | | | | | | |
|---|---|---|---|---|---|---|---|
| 1st Lateral Bending | 615 | 659 | 7% | G | 595 | 3% | G |
| Nose Block Lateral/Roll | 930 | 735 | 21% | P | 812 | 13% | P |
| Forward Cabin Lateral/ Nose Block Lateral | 990 | 858 | 13% | P | 970 | 2% | P |
| Torsion | 1310 | 1601 | 22% | P | 1325 | 1% | P |

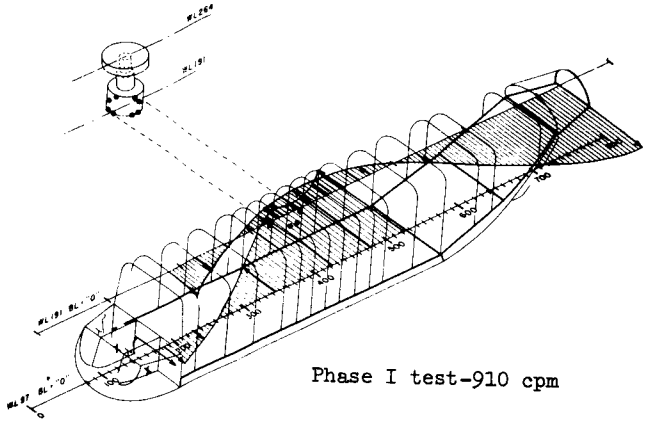

Phase I test-910 cpm

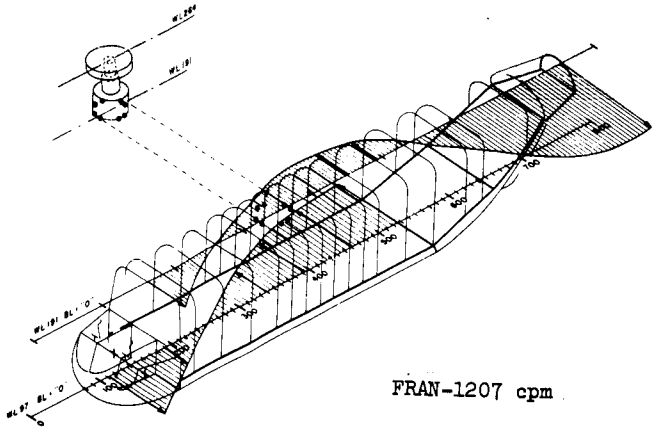

FRAN-1207 cpm

Figure 7a Correlation of First Lateral Bending Mode, Phase I - Stripped

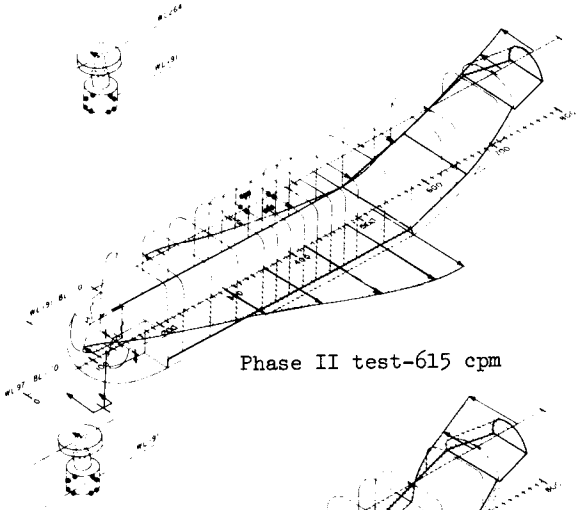

Phase II test-615 cpm

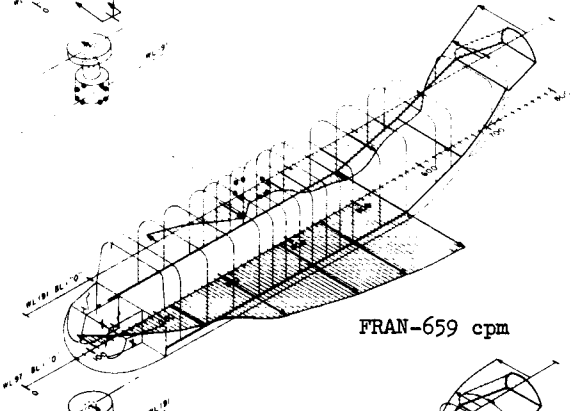

FRAN-659 cpm

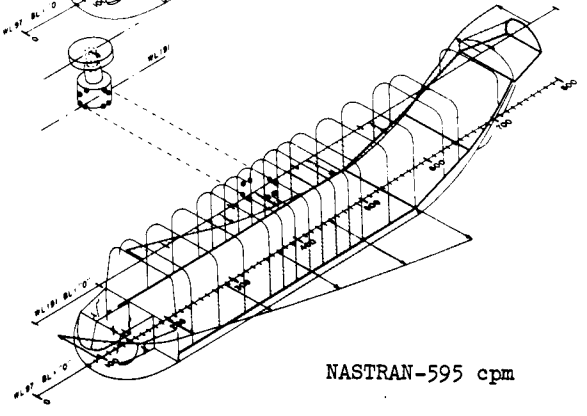

NASTRAN-595 cpm

Figure 7b Correlation of First Lateral Bending Mode, Phase II - Ballasted

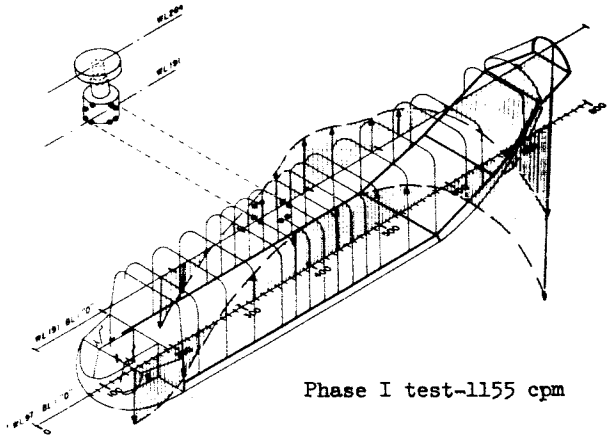

Phase I test-1155 cpm

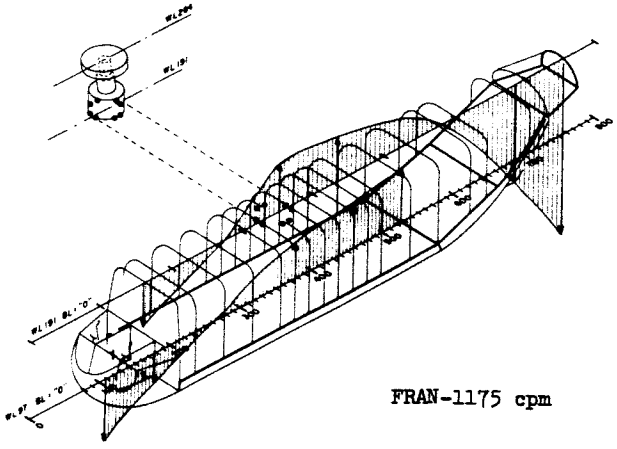

FRAN-1175 cpm

Figure 8a Correlation of First Vertical Bending Mode, Phase I - Stripped

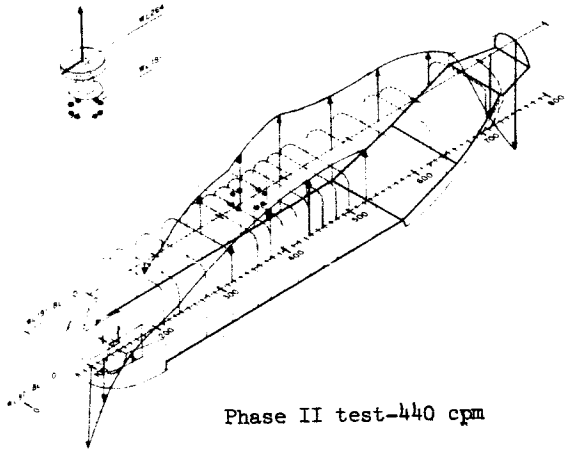

Phase II test-440 cpm

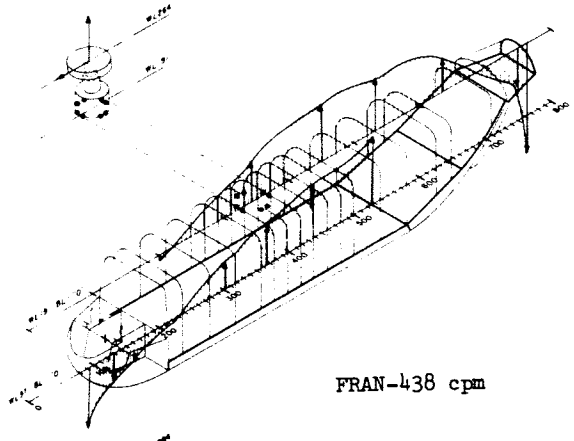

FRAN-438 cpm

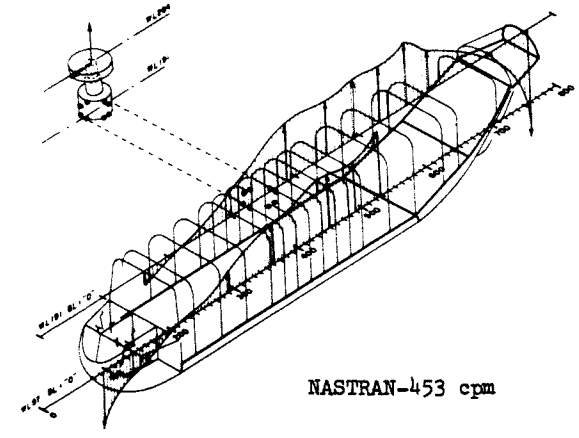

NASTRAN-453 cpm

Figure 8b Correlation of First Vertical Bending Mode, Phase II - Ballasted

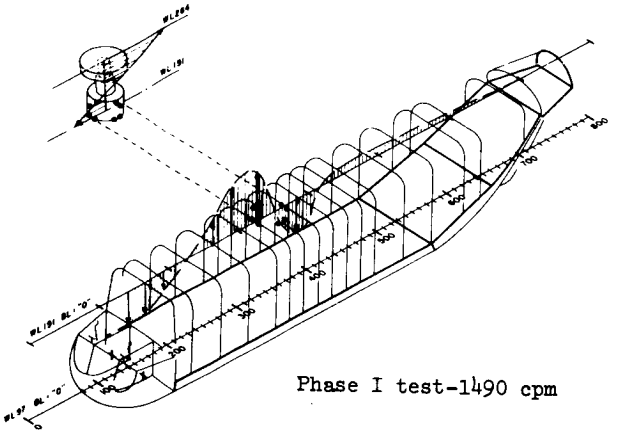


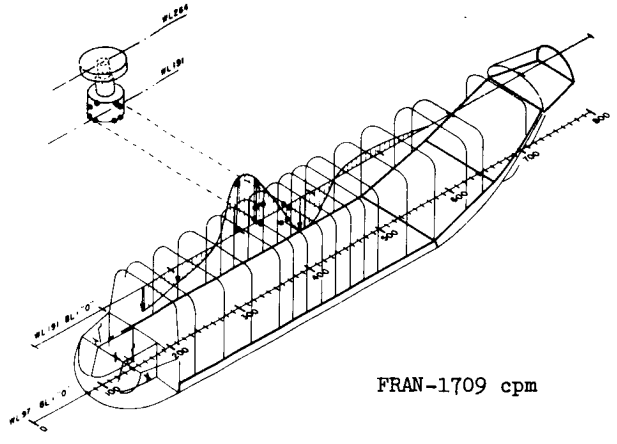


Figure 9a Correlation of Transmission Pitch Mode, Phase I - Stripped

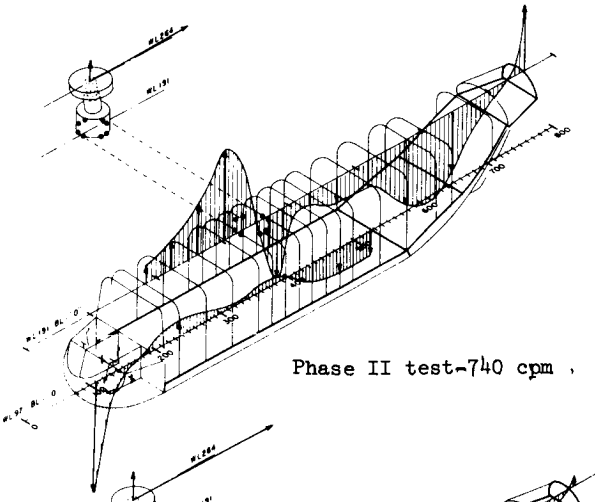


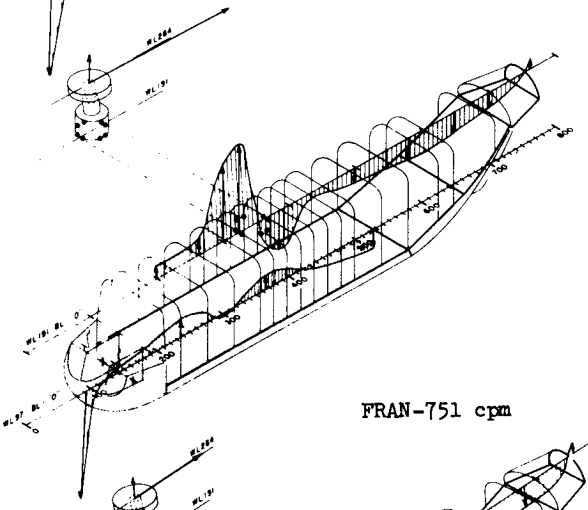


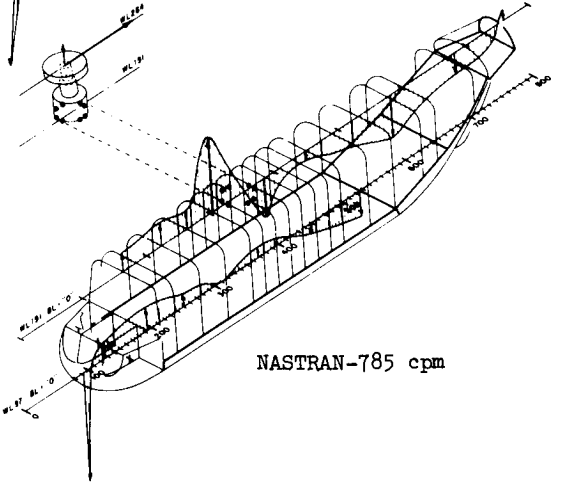


Figure 9b Correlation of Transmission Pitch Mode, Phase II - Ballasted

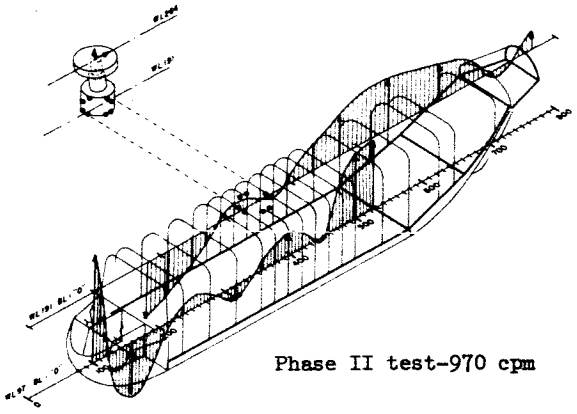

Phase II test-970 cpm

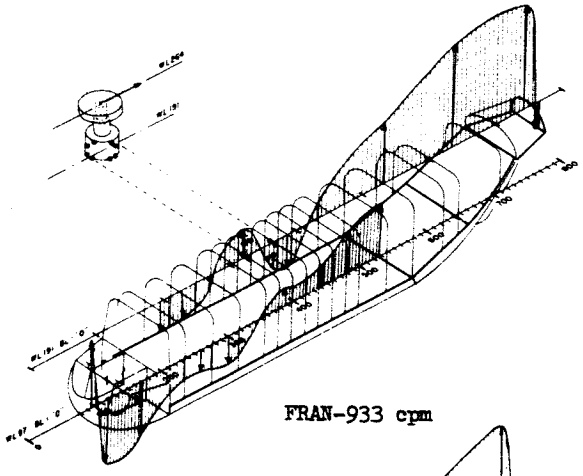

FRAN-933 cpm

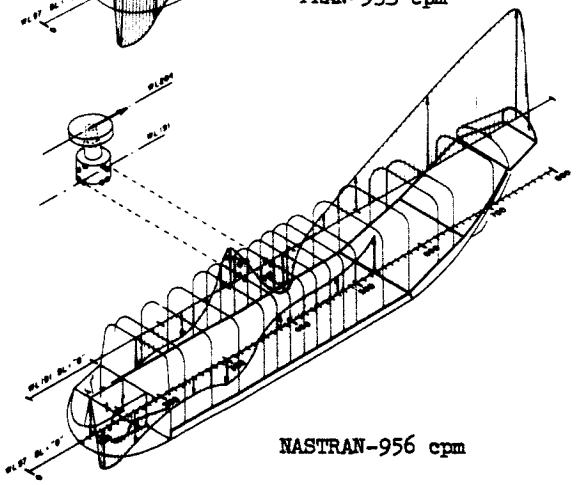

NASTRAN-956 cpm

Figure 10 Correlation Nose Block Vertical/Transmission Pitch Mode, Phase II - Ballasted

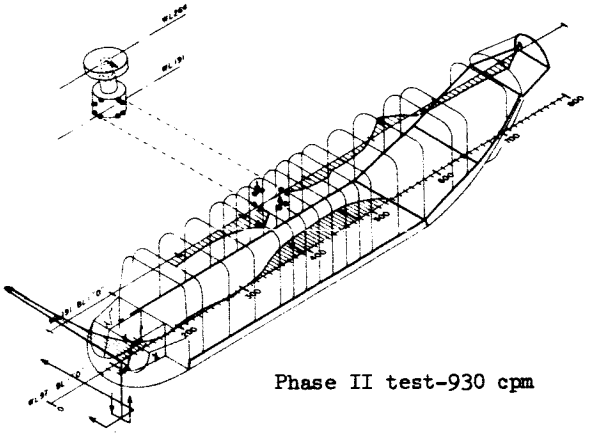

Phase II test-930 cpm

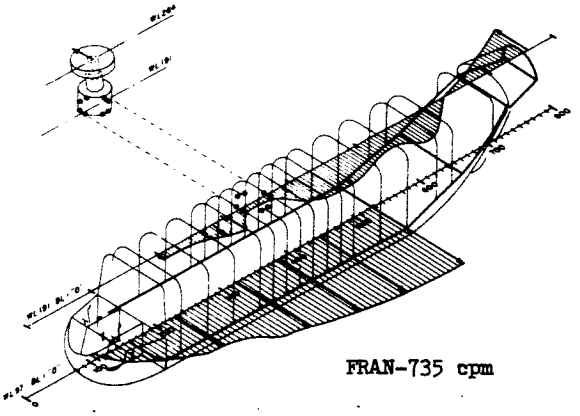

FRAN-735 cpm

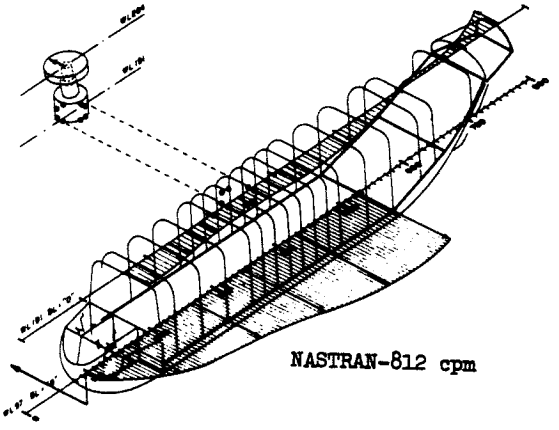

NASTRAN-812 cpm

Figure 11 Correlation of Nose Block Lateral/Roll Mode, Phase II - Ballasted

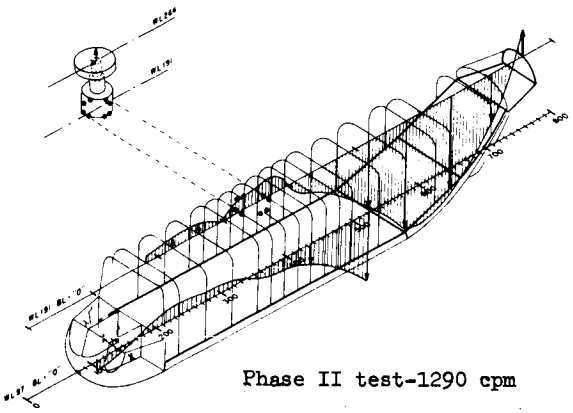

Phase II test-1290 cpm

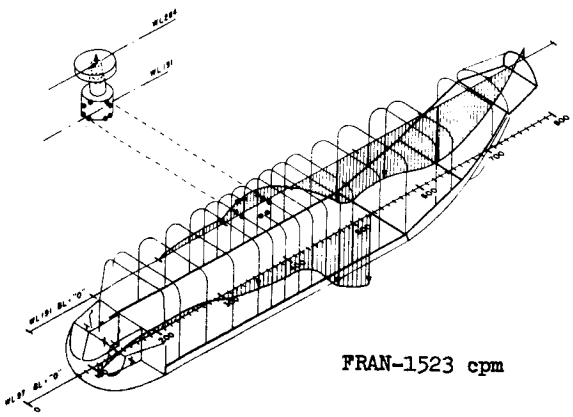

FRAN-1523 cpm

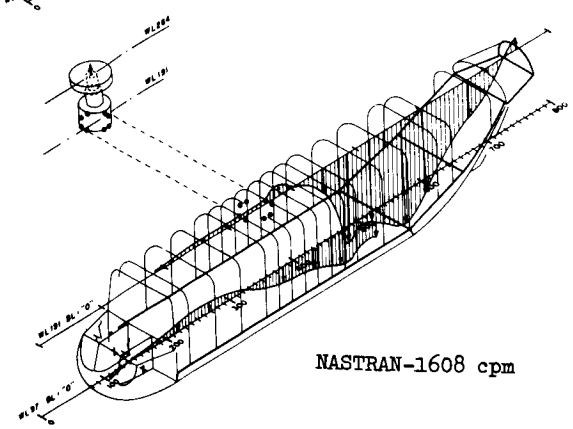

NASTRAN-1608 cpm

Figure 12 Correlation of Second Vertical Bending Mode, Phase II - Ballasted

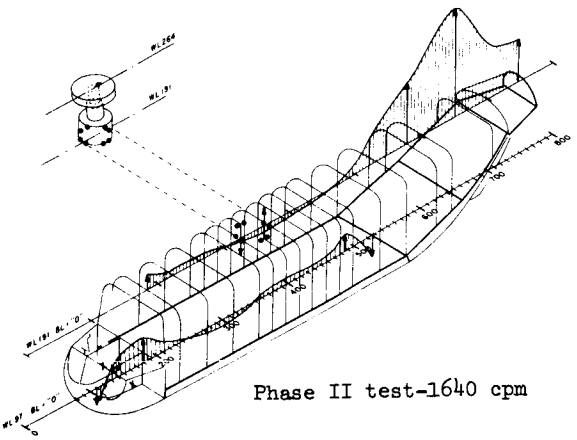

Phase II test-1640 cpm

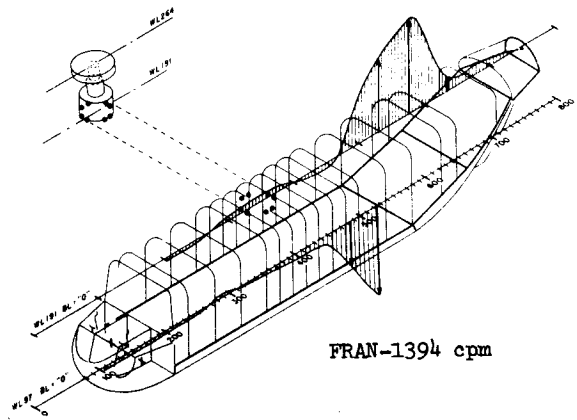

FRAN-1394 cpm

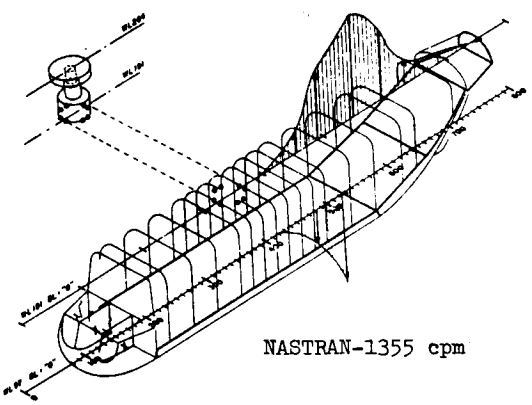

NASTRAN-1355 cpm

Figure 13 Correlation of Ramp Vertical Bending Mode, Phase II - Ballasted